

OSCILLATIONS OF HEATING PLATFORM FOR 3D PRINTING OF AGRICULTURAL DRONE PARTS

Ivan Rogovskii, Viktor Krushelnytskyi, Maksym Dombrovskiy

National University of Life and Environmental Sciences of Ukraine, Ukraine

rogovskii@nubip.edu.ua, krushelnytskyiviktor@nubip.edu.ua, dombrovskiy@nubip.edu.ua

Abstract. The article examines the fluctuations of the heating platform for a 3D printer and compares its operation before and after modernization. The main goal was to understand at which frequencies the largest vibrations occur, and how design changes affect the stability of the platform during printing. First, measurements were made in initial state. The analysis showed that the platform had rather strong oscillations in range of 10-55 Hz, especially along the Y-axis, that is, in the direction of movement of the printing carriage. The largest peaks were at frequencies of 17-18 Hz and 40-45 Hz, and the amplitude reached approximately $0.008 \text{ m}\cdot\text{s}^{-2}$. This meant that the system had several resonance zones that could negatively affect the print quality. After the modernization, when an additional guide and a second stepper motor were added, the situation changed markedly. The spectrum of oscillations became more even, and the amplitudes along the X-axis decreased almost by half, from $0.006 \text{ m}\cdot\text{s}^{-2}$ to approximately $0.003 \text{ m}\cdot\text{s}^{-2}$. Along the Y-axis, the main resonance shifted to a smaller range (13-15 Hz), and the amplitude dropped to $0.006 \text{ m}\cdot\text{s}^{-2}$. Vertical fluctuations along the Z-axis were generally very low, no more than $0.002 \text{ m}\cdot\text{s}^{-2}$, i.e. actually at the sensor noise level. In general, the modernization gave a noticeable result: oscillations decreased by about 30-50%, resonance peaks decreased, and the system itself became much more stable. This confirms that the design changes were appropriate and really affected the behaviour of the platform. These results are important because a more stable platform means fewer defects, higher print accuracy and more predictable printer performance.

Keywords: agricultural drone, 3D printing, vibration spectrum, platform, Fourier transform.

Introduction

Today, 3D printing is actively used in agricultural engineering. Thanks to this technology, it is possible to quickly create prototypes, replacement parts or entire assemblies of agricultural drones, which significantly reduces development time [1]. However, the quality of printing remains dependent on stability of the printer's mechanical components, especially during fast movements [2]. In the 3D printing process, vibrations often occur, which can cause positioning inaccuracies or deformation of the material layer [3]. Therefore, the analysis of the dynamic behaviour of printing components is important for increasing the accuracy and repeatability of results [4].

The study of 3D printer vibrations allows to identify the resonant frequencies of system, assess the influence of structural elements and propose solutions to reduce vibrations. Practical modernization of individual parts of structure allows to increase rigidity, reduce parasitic vibrations and improve the print quality [5]. Vibrations in the 3D printing process are one of key factors determining the quality, accuracy and stability of manufactured products. A number of researchers around the world are focusing on analysis of vibration sources, their impact on mechanical properties of materials, as well as methods for reducing the amplitude of vibrations in FDM printing systems [6].

Study [7] analyzed how vibrations affect the strength and elastic properties of parts printed by FDM from ABS and PETG materials. During the experiments, it was found that the vibrations that occur during printing can provoke micro-defects between individual layers, which subsequently reduces the elastic modulus and the ultimate strength of finished samples. At the same time, the author notes that products made of PET-G better tolerate dynamic loads, while ABS parts are prone to fatigue failure. In general, the study confirms that printer vibrations during layer formation have a significant impact on print quality and mechanical stability of finished components.

The researchers [8] studied the effect of system vibrations of a 3D printer on mechanical characteristics of parts manufactured by FDM from PET-G material. In work [8], experiments were conducted with the orientation of the printing direction of samples $45^\circ\times 45^\circ$ and $60^\circ\times 30^\circ$ and three printing speeds (3600, 3900 and $4200 \text{ mm}\cdot\text{min}^{-1}$). Vibration amplitudes were measured by accelerometers in three axes (X, Y, Z) on the extruder and the printer table. The results showed that the amplitude of oscillations along the Y-axis is the largest, and the minimum values were observed at orientation $60^\circ\times 30^\circ$ and the speed $3600 \text{ mm}\cdot\text{min}^{-1}$, which coincides with the maximum strength and stability indicators of samples. Thus, the authors proved that geometric orientation of layers and printing

mode directly affect the vibration response of the system, and control of these parameters allows improving the mechanical properties and reducing defects of FDM products [9].

During the modal analysis [10], it was found that the most sensitive to vibrations are the heating platform and the gantry of the print head, which have natural frequencies of about 40 Hz. Vertical vibrations of the base increased the surface roughness of parts by 85%, while the use of passive isolation reduced the relative motion between the head and the platform by 93% and improved the surface quality by 16%. This study confirmed that it is vibration of the base (in particular, the heating platform) that is the main source of defects during printing.

In the work [11], it is shown that induced vibrations can positively affect the structure of layers, improving their intermolecular adhesion. Research on the FT-5 R2 printer has proven that additional vibrations do not impair geometric accuracy but reduce porosity and increase the strength of PLA samples. The optimal excitation frequencies are considered medium, which ensure uniform distribution of material without overloading the printer mechanics [12].

The scientific paper [13] investigated the possibilities of passive vibration damping through design changes. The authors performed a series of experiments on a printer with an acrylic body and found that replacing bearings with polymer ones, reinforcing the frame with aluminium profiles, and using rubber dampers can reduce the vibration amplitude by 50-70%, which directly improves printing accuracy and surface quality.

Review [14] summarized the influence of printing parameters (laser power, speed, layer orientation) on resonant frequencies and modal shapes of metal samples. Although the study concerned metallic materials, the patterns of natural frequency changes and damping are similar for polymer FDM systems, in particular for the platform, which acts as part of the printer vibration system.

The aim of the work is to experimentally study the vibrations of the working platform of a 3D printer during the manufacture of agricultural drone parts and evaluate the effectiveness of design changes.

Materials and methods

Further research is aimed at improving the methodology for analyzing dynamic processes in the 3D printer manufacturing of agricultural drone parts, in particular, the vibrations of the heating platform during operation. The concept involves combining a sensor node based on an accelerometer with an Arduino microcontroller and software processing in the Python environment using the Kalman filter and Fourier series methods. The experimental complex used a 3D printer with CoreXY kinematic scheme (Fig. 1).

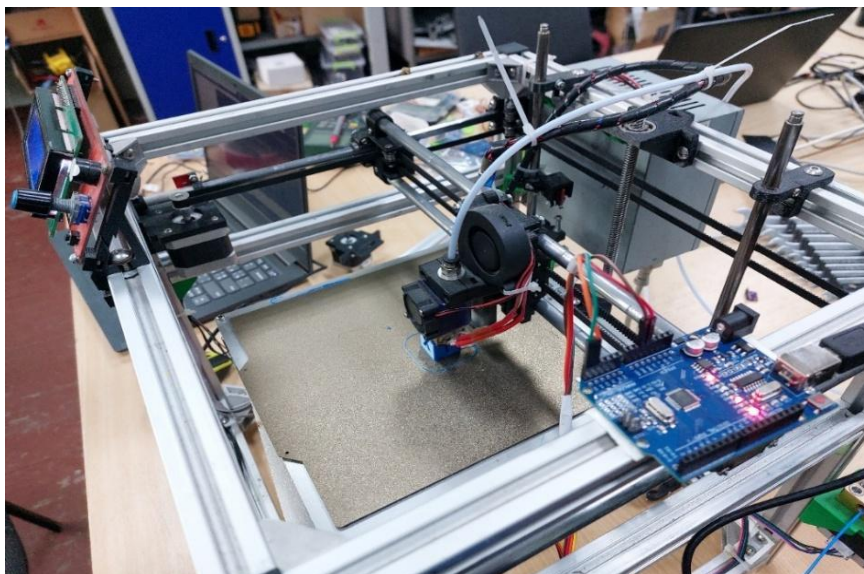


Fig. 1. Experimental 3D printer

The 3D printer with CoreXY kinematics is an additive manufacturing device in which the movement of the print head in the XY plane is carried out by two synchronized belt drives that form a planar mechanism of H-bot type. In such a system, two stationary stepper motors simultaneously control the position of the extruder: with the same rotation of motors, the carriage moves along the X-axis, and with the opposite – along the Y-axis. The combination of movements provides smooth and accurate positioning in any direction of plane. To organize the process of measuring accelerations from the MPU-9250 inertial module, a software part was developed, consisting of two components – a built-in program for the Arduino Uno microcontroller and a computer script for receiving data. The Arduino program provides sensor initialization via the I2C interface, polling at a frequency of 1 kHz and transmission of measured values to the serial port in text format. On the computer, the data is received by a specially created Python script, which reads information via the USB interface, checks the structure of received lines, and saves the results to file for further processing (Fig. 2).

```
import serial
import keyboard
import time

SERIAL_PORT = 'COM4'
BAUD_RATE = 2000000
READING_DURATION = 5 * 60

ser = serial.Serial(SERIAL_PORT, BAUD_RATE, timeout=1)

with open("datalogAcces_test_6_0.00_12042025_700Hz_5m.txt", "w") as f:
    start_time = time.time()
    last_time = start_time
    line_count = 0

    while time.time() - start_time < READING_DURATION:
        if keyboard.is_pressed('q'):
            print("Reading stopped by the user")
            break

        try:
            line = ser.readline().decode('utf-8', errors='ignore').strip()
            if line and any(char in line for char in "(){}[]"):
                f.write(line + "\n")
                line_count += 1

                if time.time() - last_time >= 1.0:
                    print(f"FPS: {line_count}")
                    line_count = 0
                    last_time = time.time()
        except UnicodeDecodeError as e:
            print(f"Decode error: {e}")
```

Fig. 2. Visualization of the developed code in the Python IDLE environment

This approach (Fig. 2) allows for reliable real-time collection of experimental data and creates basis for filtering signals, determining frequency characteristics, and statistical processing of results. This greatly facilitates further work with large volumes of measurements. The script also provides for possibility of real-time visualization of signal fragments, which allows to control the quality of reading during the experiment and, if necessary, adjust the research conditions. Such flexibility makes the data collection system convenient for iterative experiments and increases the reliability of the results obtained.

Results and discussion

To implement signal filtering based on the general linear model, a program code was created in the Python environment. The program structure involves the creation of a separate class KalmanFilter1D (Fig. 3), which implements the basic stages of prediction, calculation of the Kalman coefficient, correction of the estimate and update of the error. The algorithm operates recursively, that is, for each new measurement of the signal, a previous state estimate is used, which allows for a quick response to a change in the dynamics of oscillations.

After filtering, the results were visualized in the form of three graphs – for each axis separately (Fig. 4). Each of them is marked with blue or green raw data, and red – filtered values after processing

by the Kalman filter. Let us consider the graphs in more detail by approximating the study interval from 300 seconds to 2 seconds. The graphs clearly show a decrease in the amplitude of high-frequency noise and the separation of the main periodic component of oscillations, which corresponds to real movement of the platform. After filtering the signals, a uniform change in acceleration is ensured without impulse jumps characteristic of digital sensor interference. Such local scaling of the graphs allows us to more accurately assess the signal structure and make sure that the Kalman filter does not distort the physical behaviour of the system but only dampens the noise. It is clearly visible that the filtered curve repeats general shape of the output signal, but at the same time is much smoother and more stable. This confirms the correctness of filter parameter settings and the effectiveness in analyzing fast oscillatory processes. Within a 2-second interval (Fig. 4), it is clearly seen that the Kalman filter effectively suppresses random high-frequency oscillations on all three axes and preserves the real shape of the useful signal. Thus, the use of the filter allows to obtain a high-quality signal suitable for further spectral analysis.

```
import numpy as np
import matplotlib.pyplot as plt
import re

class KalmanFilter1D:
    def __init__(self, q=1e-5, r=1e-2, initial_estimate=0.0, initial_error=1.0):
        self.q = q
        self.r = r
        self.x = initial_estimate
        self.p = initial_error

    def filter(self, data):
        result = []
        for z in data:
            self.p = self.p + self.q
            k = self.p / (self.p + self.r)
            self.x = self.x + k * (z - self.x)
            self.p = (1 - k) * self.p
            result.append(self.x)
        return np.array(result)
```

Fig. 3. Implementation of the Kalman filter in Python

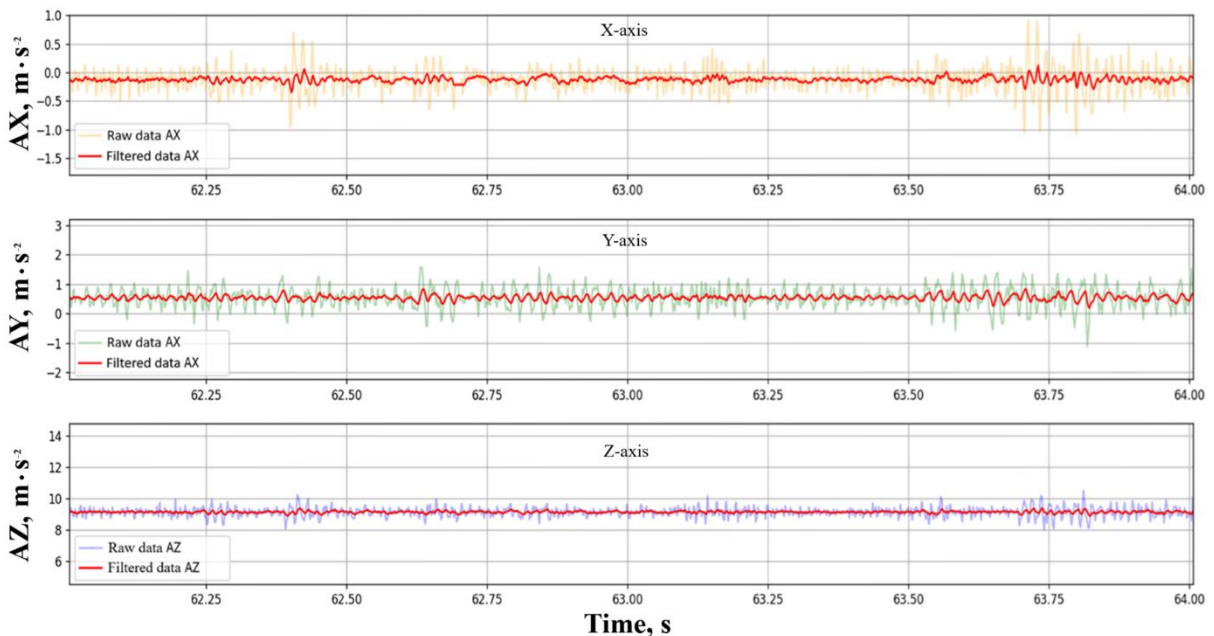


Fig. 4. Fragment of experimental acceleration data from 62 to 64 seconds of the experiment along the X, Y, Z axes

The signal without filtering (yellow line) is characterized by high-frequency oscillations with an amplitude of about $\pm 1.5 \text{ m}\cdot\text{s}^{-2}$. After filtering (red line), a significant smoothing of the signal is observed and only the main low-frequency component is preserved. This indicates effective suppression of

random noise and stability of the platform in the transverse direction. After filtering the data, a spectral analysis of the filtered signals (Fig. 5) was performed to determine the frequency characteristics of the heating platform oscillations after modernization. The Fourier transform was applied to data along all three axes – X, Y, Z, which allowed us to estimate the amplitude distribution in frequency domain and identify the dominant frequencies of the system resonant oscillations.

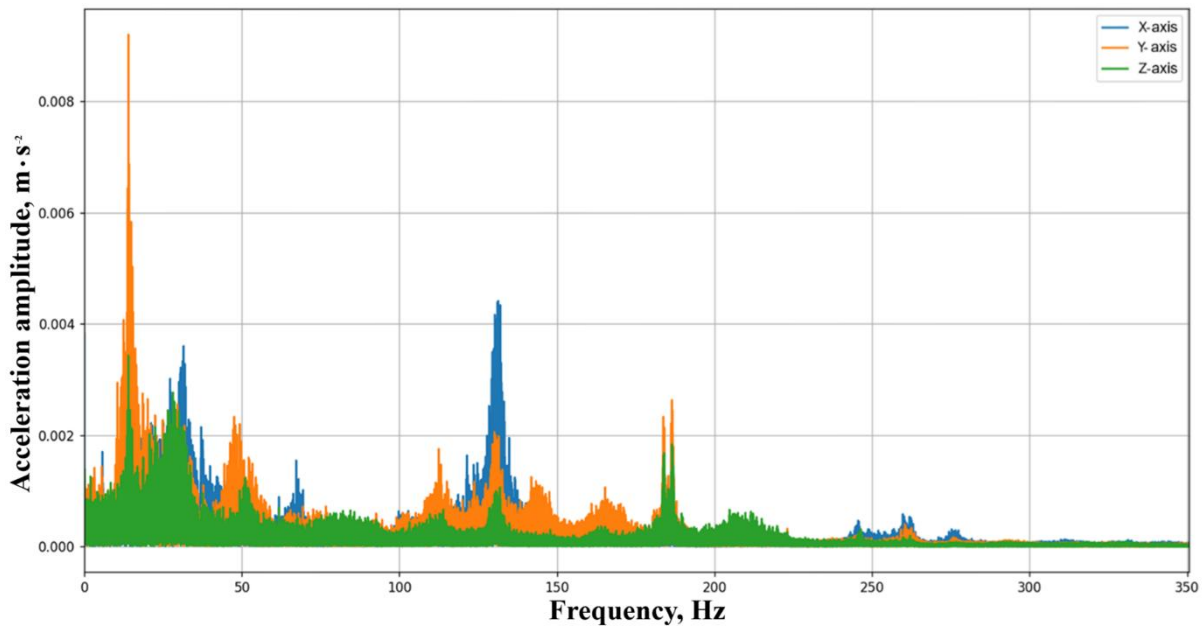


Fig. 5. Amplitude-frequency spectrum graph, frequency 0-350 Hz

Along the X-axis (Fig. 5), the spectrum shows several pronounced peaks in the range of 25-35 Hz with maximum amplitude of about 0.003-0.0035 $\text{m}\cdot\text{s}^{-2}$. This may correspond to natural vibrations of horizontal frame elements. The intensity of peaks is lower than in the previous experiment, which indicates an increase in stiffness in transverse direction.

Along the Y-axis (Fig. 5), the dominant peak is observed at 13-15 Hz with an amplitude of about 0.005-0.006 $\text{m}\cdot\text{s}^{-2}$, which corresponds to fundamental frequency of operating vibrations during the movement of the print head. The second, less pronounced maximum is located in the 35-40 Hz zone, which may be a harmonic of fundamental resonance or consequence of periodic loading of drive. In general, the energy level along the Y-axis has significantly decreased compared to the initial state, but the Y direction remains the most active in terms of vibration energy.

Along the Z-axis (Fig. 5), the amplitudes of oscillations in vertical direction do not exceed 0.0015-0.002 $\text{m}\cdot\text{s}^{-2}$, which is within the background level. The main activity is observed in the 15-25 Hz zone, synchronous with movements along the Y-axis, which indicates a kinematic connection between the vertical platform and the movement of the print head. Above 40 Hz, the amplitudes disappear, i.e. high-frequency resonances are absent.

Conclusions

1. The system demonstrated increased activity in the range of 10-55 Hz, where the main resonant oscillations were observed. The highest acceleration values were recorded along the Y-axis – the direction of movement of the printing carriage. Pronounced peaks at 17-18 Hz and 40-45 Hz (up to 0.008 $\text{m}\cdot\text{s}^{-2}$) indicate presence of two resonant zones that affected the stability of the platform.
2. The addition of the guide axis and second stepper motor resulted in more uniform spectrum of vibrations. On the X-axis, the amplitudes were halved – from 0.006 to 0.003-0.0035 $\text{m}\cdot\text{s}^{-2}$, indicating an increase in stiffness. On the Y-axis, the resonance shifted to 13-15 Hz region, and amplitude decreased to 0.005-0.006 $\text{m}\cdot\text{s}^{-2}$.
3. Vertical vibrations along the Z-axis do not exceed 0.002 $\text{m}\cdot\text{s}^{-2}$ – practically the background level. This means effective vibration damping and the absence of parasitic resonances. The appearance of shift in resonant frequency to lower region indicates a change in the unit's own dynamic parameters,

which confirms the effectiveness of additional guides and drive. In general, the results of spectral analysis demonstrate that modernization improved the platform behaviour under load and created better conditions for stable and high-quality 3D printing details of the agrodrome.

Acknowledgements

This paper was supported by the HEI-COPILOT project within the EIT HEI Initiative “Innovation Capacity Building for Higher Education”, funded by the European Union.

Author contributions

Conceptualization, I.R.; methodology, I.R. and V.K.; software, M.D.; validation, I.R. and V.K.; formal analysis, I.R. and V.K.; investigation, I.R., V.K. and M.D.; data curation, I.R., V.K. and M.D.; writing – original draft preparation, M.D.; writing – review and editing, I.R. and V.K.; visualization, I.R. and V.K.; project administration, I.R.; funding acquisition, I.R. All authors have read and agreed to the published version of the manuscript.

References

- [1] Rogovskii I., Kotliarov V., Bondarenko V., Chen Gaojiang, Li Zehao. Engineering and security management of Smart technology of agrotechnics of crop production. Contributions to Finance and Accounting, part F4082, 2024, pp. 93-102, DOI: 10.1007/978-3-031-75960-4_10
- [2] Zimu G., Benjamin J., Sipei Z. Enhancing 3D printing quality: active vibration control for FDM in challenging environments. Inter-noise and Noise-con Congress and Conference Proceedings, vol. 272(4), 2025, pp. 946-954, DOI: 10.3397/IN_2025_1074209
- [3] Thuy C., Tan N., Hyunsang Y., Jihoon W. A review of vibration analysis and its applications. Heliyon, vol. 4, 2024, pp. e26282. DOI: 10.1016/j.heliyon.2024.e26282
- [4] Kati H., He F., Khan M., Gokda H. Effect of printing parameters on the dynamic characteristics of additively manufactured absbeams: an experimental modal analysis and response surface methodology. Polymer, vol. 17, 2025, pp. 1615. DOI: 10.3390/polym17121615
- [5] Golub G., Tsyvenkova N., Chuba V. Determining the influence of design features in agrivoltaics systems on tracking efficiency. Eastern-European Journal of Enterprise Technologies, vol. 3, 2025, pp. 14-22. DOI: 10.15587/1729-4061.2025.329837
- [6] Agarwal V. Vibrational analysis of 3D printed components. International Journal of Scientific Research and Engineering Development, vol. 4(6), 2021, pp. 593-598. <https://surl.li/lrhymf>
- [7] Kam M., Saruhan H., İpekçi A. Investigation the effect of 3D printer system vibrations on surface roughness of the printed products. Düzce Üniversitesi Bilim ve Teknoloji Dergisi, vol. 7(2), 2019, pp. 109-119. DOI: 10.29130/dubited.441221
- [8] Jensen N.J., Parker G.G., Blough J.R. (2024). Base vibration effects on additive manufactured part quality. Experimental Techniques, vol. 48, 2024, pp. 159-170. DOI: 10.1007/s40799-023-00629-1
- [9] Dei R.J., Keles O., Viswanathan V. Fused deposition modeling with induced vibrations: a study on the mechanical characteristics of printed parts. Applied Sciences, vol. 12(18), 2022, pp. 9327. DOI: 10.3390/app12189327
- [10] Białas, K., Dymarek, A., Dzitkowski, T. (2023). Impact of 3D printer vibration reduction on the quality of its printout. International Journal of Modern Manufacturing Technologies, vol. 15(2), 2023, pp. 79-90. DOI: 10.54684/ijmmt.2023.15.2.79
- [11] Sinan K.I. Influence of steel fiber (SF) addition on the enhancement compressive strength of pure gypsum. Materialstoday, vol. 3, 2023, pp. 156-183. DOI: 10.1016/j.matpr.2023.11.119
- [12] Haishen J., Liu Y., Li W. Parameter optimization and spatio-temporal distribution of material for variable trajectory combined equal-thickness screen. Powder Technology, vol. 1, 2024, pp. 119590. DOI: 10.1016/j.powtec.2024.119590
- [13] Gabstur P., Kocisko M., Torok J., Kascak J. Enhancement of primary profile surface quality in fff printing through vibration monitoring and active control. Appl. Sci. vol. 15, 2025, pp. 11346. DOI: 10.3390/app152111346
- [14] Bharat Y., Aayush A., Prokop A. Influence of printing parameters on the mechanical behavior of 3D-printed SS316L parts manufactured using laser hot wire directed energy deposition. The International Journal of Advanced Manufacturing Technology, vol. 134, 2024, pp. 3281-3292. DOI: 10.1007/s00170-024-14308-x